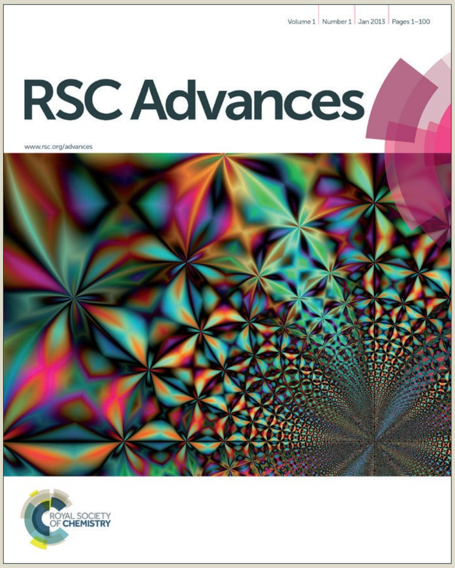

ROYAL SOCIETY OF CHEMISTRY

www.rsc.org/advances

Journal Name

COMMUNICATION

Titania nanotubes infiltrated with conducting polymer PEDOT modified by Prussian Blue – a novel type of organic-inorganic heterojunction characterised with enhanced photoactivity

Received: 00 January 20xx,
Accepted: 00 January 20xx

DOI: 10.1039/x0xx00000x

www.rsc.org/

K. Siuzdak[a], M. Szkoda[b], J. Karczewski[c], J. Ryl[d], A. Lisowska-Oleksiak[b]

The highly ordered p-n heterojunction was formed based on titania nanotubes containing conducting polymer with Prussian Blue matrix. The study demostrates, for the first time, cases when composite based on titania arrays scaffolding and Prussian Blue embedded in PEDOT exhibits reversible Fe^{II}/Fe^{III} redox activity. Highly enhanced photoactivity and capacitance of the obtained material are depicted in comparison to pristine titania. To the best of our knowledge this is first report showing heterojunction with titania nanotubes containing redox active species that may take part in efficient photocurrent generation.

Highly ordered titania nanostructures are currently regarded as a promising material for sensors, electrochromic devices, solar cells and supercapacitors[1], owing to their relatively simple and highly-controlled anodization procedure. However, the usage of titania nanotubes (NTs) as a photoelectrode material is limited to the UV illumination as a result of the wide band gap energy[2]. Thus, many efforts are undertaken to shift its activity towards the visible wave range, e.g. metal or non-metal doping[3], integration with other metal oxides[4] or deposition of conducting polymer (CP).[5] In the case of different approaches concerning TiO_2NT covered by CPs, many drawbacks were identified, such as uneven polymer distribution[6] and complicated synthesis requiring protocol, e.g. initial TiO_2 surface modification[7] or electrode illumination (photo-electropolymerisation)[8]. In regard to composite photoactivity, only two times higher enhancement of photocurrent after polymer deposition was reached[9,10,11] at most, or its photostability was unsatisfactory[12]. Another interesting approach leading to titania activation in the visible range concerns the deposition of different metal hexacyanometallates - mainly iron, cobalt or zinc analogues[13]. For Mehcf-modified TiO_2, the photoelectrochemical characterisation[14] and photoelectrochromic behaviour have been investigated[15]. The obtained results showed that, for instance iron hexacyanoferrate species anchored on the titania surface could play a crucial role in efficient photoactivity, preventing recombination of the electron-hole pair in TiO_2.[16] Despite many approaches towards enhancement of titania NTs activity under irradiation which were proposed concerning both polymer electrodeposition in the presence of different counter ions' sources (Bu_4NBF_4[17], SDBS[18], $LiClO_4$[19]) or sensibilization by various ferricyanide derivatives[20], no combinations of both attempts were achieved.

Here, the study shows the preparation of inorganic-organic heterojunction where ordered titania nanotubes were infiltrated by nanostructure combining poly(3,4-ethylenedioxythiophene) (PEDOT) and iron hexacyanoferrate (Fehcf, Prussian Blue). For the first time, composite with the use of titania nanotubes exhibits reversible redox reaction that is attributed to both high and low spin Fe^{II}/Fe^{III} redox couple of Prussian blue activity[21.] The study reports on the highly improved electrochemical activity of the obtained material as well as on the generated photocurrent. The detailed experimental conditions for material preparation and its characterisation are given in ESI. In general, ordered titania arrays were produced *via* two step anodization performed at electrolyser voltage of 40 V for 2 h each, followed by calcination in 450°C. Finally the samples underwent a hydrogen plasma treatment for 1h[22]. The deposition of polymer was realized during potentiostatic polymerisation in three electrode cell in the presence of $Fe(CN)_6^{3-/4-}$ ions under the potential of 1.6 V consuming charge of Q = 30 (small polymer amount) or Q = 300 mC cm^{-2} (excess of polymer amount). Polymer film $pEDOT/Fe(CN)_6^{4-/3-}$ obtained onto TiO_2NT support was then subjected to potentiodynamic polarisation in $FeCl_3$ solution according to the procedure described previously[23]. Characterisation of material using different spectroscopic techniques and electrochemical studies

---

[a] Centre for Plasma and Laser Engineering, The Szewalski Institute of Fluid-Flow Machinery, Polish Academy of Science, Fiszera 14, 80-231 Gdańsk, Poland
[b] Department of Chemistry and Technology of Functional Materials, Chemical Faculty, Gdańsk University of Technology, Narutowicza 11/12, 80-233 Gdańsk, Poland
[c] Faculty of Applied Physics and Mathematics, Gdańsk University of Technology, Narutowicza 11/12, 80-233 Gdańsk, Poland
[d] Department of Electrochemistry, Corrosion and Materials Engineering Chemical Faculty, Gdańsk University of Technology, Narutowicza 11/12, 80-233 Gdańsk, Poland

† Electronic Supplementary Information (ESI) available: [details of any supplementary information available should be included here]. See DOI: 10.1039/x0xx00000x

were performed for the pristine titania and composite containing small polymer amount (consumed charge of 30 mC cm^{-2}) and all potentials were given *vs.* Ag/AgCl/0.1M KCl used as reference electrode in three electrode cell. Fig. 1a shows SEM images of titania nanotubes whereas the composite material with small and the excess of polymer material are given in Fig. 1b and 1c, respectively. The titania layer (Fig. 1a) is composed of regular nanotubes with internal radius of 50 nm, wall thickness of 25 nm and length of 2.5 μm. In the Fig. 1b), in the nearest vicinity of the vertical walls some small irregular species may be identified. Taking into account consumed charge and previous experimental data[23] the thickness of this polymeric layer is c.a. 3 nm. Therefore, SEM imaging does not sufficient for clear distinction between pristine titania and titania modified with a small polymer amount. However, when a large excess of pEDOT:Fehcf is deposited (see Fig. 1c), it covers TiO_2NT completely and only at some crack sites, a tubular structure is unsheathed as it is indicated in Fig. 1d registered at higher magnification of area pointed in Fig. 1c. Energy-dispersive X-ray spectroscopy (EDX) inspection performed in different locations at the surface and across the layer of the composite sample shows that apart from Ti and O, sulphur, iron and nitrogen atoms are present at the surface region as well as at the bottom of the tube. The atomic content of elements in composite with the small polymer amount (Q = 30 mC cm^{-2}) was found as follows: Ti (16.0 at %), O (33.7 at %), C (42.1 at %), N (2.7 at %), Fe (0.6 at %) and S (4.9 at %). Thus, the ratio of pEDOT and PB could be estimated roughly to 4 pEDOT mer units for 1 PB unit each combining two iron atoms. The identification of the titania crystalline phase and CPs with embedded inorganic species was performed additionally by Raman and X-ray photoelectron spectroscopy.

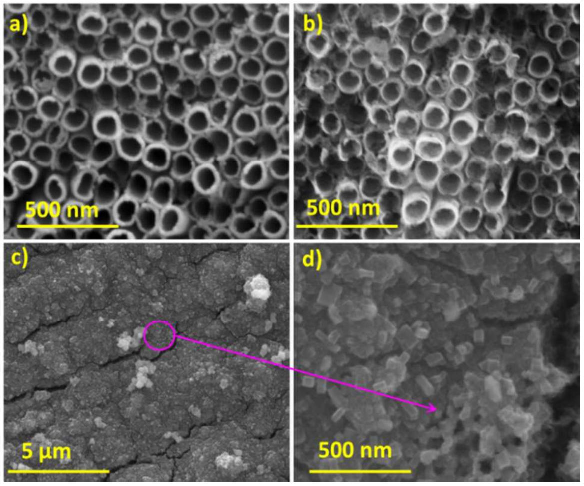

Fig. 1. SEM image of TiO_2 (a) and composite with a small amount (Q = 30 mC cm^{-2}) (b) and a large excess (Q = 300 mC cm^{-2}) (c,d) of deposited pEDOT:Fehcf.

Similarly to EDX results, the XPS analysis of composite shows that heterojunction consists of C, S, O atoms originating from polymer, and C, N, Fe atoms which are typical only for PB species are shown in Fig. 2, whereas the XPS spectra found for the other elements are given in ESI (Fig. S4). The binding energies for iron found in the range of 708-711 eV are known for compounds containing iron at valence states Fe^{II} or/and Fe^{III}. The location of registered A and B maxima are similar for Fe2$p_{3/2}$ in pristine Prussian Blue[24]. However, the location of B peak is shifted towards higher energy values when compared to pure PB as in the previous report[25]. The main peak could be then ascribed to Fe$^{(III)}$-(NC), whereas the smaller one could be attributed to Fe$^{(II)}$-(CN). The main core-level peaks of N1*s* (see Fig. 2b) are centred at 397.5, 399.2 and 401.6 eV. Peak A originates from nitrogen present in cyanide groups in Fehcf and peak B could result from the chemically new configuration formed by direct interaction between polymer and hexacyanoferrate ions.[25] The weakest signal C might be ascribed to the M-C≡N-Ti surface complexes[26]. The spectrum registered for S2*p* (see Fig. S4a) gives two maxima that were deconvoluted into doublets. Peak assigned as A is attributed to sulphur in C-S bond of thiophene ring present in pEDOT chains, whereas B signal could be identified as S in higher valence. This signal may result from direct interaction between polymer chains *via* S and Fe atoms from Fehcf[25]. The peaks found in Ti2*p* (Fig. S4b) region were localized at 459.2 and 464.94 eV. They are attributed to Ti(IV) in anatase. The peaks corresponding to O1*s* (Fig. S4c) spectrum were identified at 530.4, 531.4 and 533.0 eV. The highest one results from titania lattice oxygen. The next one (B) could be assigned to O in water molecules as it is known that they are incorporated into the metal hexacyanoferrate structures[27]. The last signal (marked as C) is attributed to oxygen in the C-O arrangement present in the polymer chain. Concerning the carbon region, the registered C1*s* (Fig. S4d) signal could be fitted by four single peaks located at 284.7, 285.54, 286.6 and 288.87 eV. The most intensive signal located at 284.7 eV could be attributed both to C-C, while the peak found at 285.54 eV may be assigned to C-S arrangement[28]. The next one, at 286.6 eV, is typical for C-O-C in ether ring of pEDOT, whereas the smallest one (288.87 eV) could be rather ascribed to carbon atoms in the CN group[29]. It should also be noted that apart from the polymer chain, the source of carbon could be identified partially as titania surface contamination originating from an anodization process performed in an organic electrolyte[3].

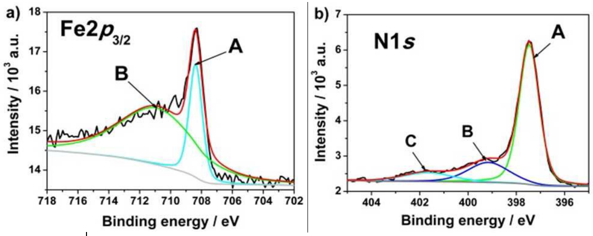

Fig. 2. XPS spectra for: a) Fe2$p_{3/2}$ and b) N1*s* of TiO_2/pEDOT:Fehcf (Q = 30 mC cm^{-2}).

The Raman spectra recorded for heterojunction and only for TiO_2NT support are presented in Fig. 3a. The active modes typical for anatase crystalline phase[30] were observed for both n-type semiconductor and composite material. After polymer deposition, a signal occurs which may be assigned to vibrations in thiophene ring (1433 cm^{-1}) and in polymer chains (1495 cm^{-1} and 1561 cm^{-1}), and in single bonded carbons in both polymer chain (1366 cm^{-1}) and in thiophene ring (1267 cm^{-1})[31]. Furthermore, at wavenumbers: 442, 571 and 988 cm^{-1} the oxyethylene ring deformations could be identified and confirmed pEDOT presence. In order to follow the change in optical properties upon polymer deposition, the UV-vis spectra were measured (see Fig. 3b). For titania, strong absorbance is observed mainly in the UV region that results from the wide bandgap energy (E_{bg}=2.98 eV). The very wide band observed in the range of 400-700 nm results from the sub-band gap states caused by the unusual structure of TiO_2 nanotube, saturation of oxygen vacancies or other defects[3]. The absorbance spectrum recorded for composite exhibits a shape similar to titania, but characterised with much highly improved absorbance ability above 450 nm, that could be attributed to the π-π* transitions in the oxidized polymer matrix. Another reason for visible light absorption is metal-ligand charge transfer of $Fe(CN)_6^{3-}/Fe(CN)_6^{4-}$[32]. Additionally, as it is known, cyanoferrate anions could be easily chemisorbed onto the surface of titanium dioxide leading to the formation of $Fe(II)(CN)_5$-C≡N-Ti(IV)[33]. Such an arrangement is characterised by broad absorption in the visible range resulting from metal-metal charge transfer (MMCT) ($Fe^{II} \rightarrow Ti^{IV}$) and could have some influence onto the absorbance ability of the whole heterojunction. In order to investigate the electrochemical properties of the formed heterojunction, cyclic voltammetry (CV) curves were registered (see Fig. 4a).

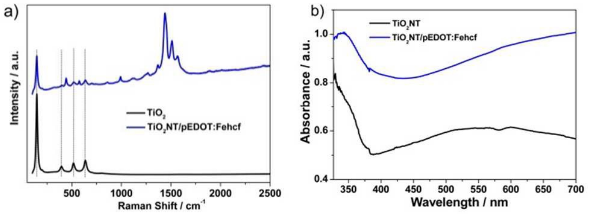

Fig. 3. a) Raman spectra and b) absorbance spectra for titania and TiO_2NT/pEDOT:Fehcf material (Q = 30 mC cm^{-2}).

The materials used as working electrodes: TiO_2NT and TiO_2NT/pEDOT:Fehcf were polarized from -0.4 V up to +0.9 V For TiO_2NT electrode, recorded CV is characterised with capacitive behaviour. The electroactivity is low and that could be identified with the oxidation/reduction of surface hydroxyl groups[34]. In the case of pEDOT:Fehcf deposited onto ordered titania, two reversible sharp (+0.15 and +0.13 V) oxidation and reduction peaks are observed respectively. They are attributed to the $Fe(CN)_6^{3-/4-}$ activity and were previously shown for pEDOT:PB hybrid[28]. As it was reported, at a potential of +0.15 V PB (blue) is reduced to Everitt's salt whereas at +0.55 V the peaks observed were less sharp and lower. They had less symmetric behaviour than the signals observed below 0.2 V and could be identified as a prestep of formation of Berlin Green (BG) as shown by Ricci *et al*[35]. This peak is cathodically shifted when compared to sharp, electrochemical activity of pure Fehcf and it may be caused by the electrochemical nature of titania acting as a pEDOT:Fehcf support. According to Itaya *et al*[36], this potential activity comes from trivalent high-spin iron ions Fe^{III}, whereas low spin iron activity is negligible. At the potential above 0.7 V, the growing current reaches the anodic wave of electrolyte decomposition. The CV exhibits also a typical rectangular shape which is characteristic for pseudocapacitive behaviour of conducting polymer[37]. Huge difference between charging current of TiO_2NT and composite could be also caused by the three-dimensional architecture of titania substrate that is infiltrated by the CP matrix. The photoactivity of heterojunction was verified as a current generated under simulated solar light irradiation (see Fig. 4b), when electrode was polarized up to 0.4 and 0.8 V. These potentials were selected according to the electrochemical activity exhibited on CV curves. In the case of titania, the photocurrent reached 61 μA cm^{-2} at 0.8 V and 40 μA cm^{-2} at 0.4 V. However, when the composite heterojunction was illuminated, the generated current reached 298 and 140 $μAcm^2$ at 0.8 and 0.4 V, respectively. The current value registered in the dark for TiO_2NT was always below 1 $μAcm^{-2}$, whereas for TiO_2NT /pEDOT:Fehcf was observed on the level of 10 $μAcm^{-2}$, and resulted from the capacitive behaviour of the polymer. Denoting photocurrent as the difference between the current registered under illumination and in the dark, after pEDOT:Fehcf deposition the photocurrent increased to 4.72 (at 0.8 V) or 3.25 times (at 0.4 V) when compared to TiO_2NT and is also much higher comparing to titania infiltrated with polymer without redox centres.[22] Furthermore, it should be noted that when 0.4 V was applied, the chronoamperometry (CA) curve of TiO_2NT/pEDOT:Fehcf exhibited spikes upon light illumination, but the current rapidly stabilized, whereas at 0.8 V the typical square shape transients were registered. It can be inferred that the recombination process does not occur at a significant rate at higher anodic potential applied to the working electrode[38]. The impact of the electrode potential on the current density value and CA shape may be related with the oxidation state of the polymer[39] and with the efficiency of charge separation resulted from electrical field generated in the space charge layer. Moreover, during the whole CA measurement period, the current registered both under illumination and in the dark periods is registered at the same level and indicates high stability and photocorrosion resistance of titania The obtained photocurrent enhancement observed for TiO_2NT/pEDOT:Fehcf composite could be attributed to the several factors. First, it is related to the absorbance ability of the polymer resulting from the π-π* transitions. According to Liang *et al.*[40], during illumination of polymer-titania NTs junction the adsorbed photon promotes electron transfer from the ground to the excited state. If e-h recombination does not proceed immediately, they are trapped in metastable states or migrate through a tubular structure towards the electrode. Here, TiO_2NT structure provides a straight path for electron movement and the close contact between the polymer matrix and the tubular structure facilitate charge collection. Apart from the absorbance ability of polymer and ordered titania morphology, the relative position of energy bands of inorganic and organic elements plays a very important role. In Fig. S5, schematic representation of the energy diagram of heterojunction is depicted. The lowest unoccupied molecular orbital (LUMO) level is situated in an energetically higher position than the conduction band edge of TiO_2NT. Thus, when the junction is illuminated, the excited electrons of pEDOT:Fehcf in the highest occupied molecular orbital (HOMO) level could move to the LUMO and then the electronic transport of charge carriers could easily occur from polymer towards TiO_2NT[41]. Additionally, the applied external potential would lead to band bending and facilitate charge separation and their transfer from an organic to inorganic part and thereby improve charge separation or the faradaic process[42]. Separated holes of TiO_2NT can enter the HOMO of pEDOT:Fehcf and then could be efficiently extracted to the interface between photoanode and aqueous electrolyte and consumed to oxidized H_2O. Additionally, other destinations for holes could be the low spin iron centres[43]. Other factors that play an important role in photoactivity enhancement are related to the presence of Prussian blue centres at the surface of titania. It is highly possible that during the first stage of polymer formation, feriicyanide ions become bound to the titania surface *via* axial cyanide bridge: Ti-C≡N-Fe[43]. This type of bonding constitutes a good platform for strong electronic coupling between surface species and a semiconductor[44]. As discussed above, the efficient generation of photocurrent possesses a complex nature and needs further studies.

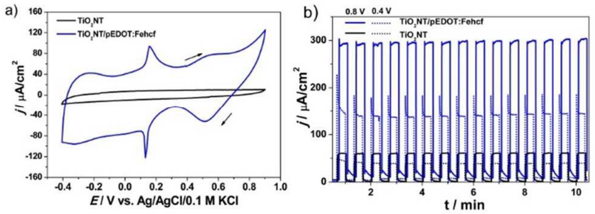

Fig. 4. a) The cyclic voltammetry and b) chronoamperometry curves recorded in 0.5 M K_2SO_4 for titania and TiO_2/pEDOT:Fehcf (Q = 30 mC cm^{-2}).

In summary, a new synthetic method and preliminary results concerning organic-inorganic heterojunction containing highly ordered titania nanotubes and inorganic redox centres embedded in pEDOT is presented. The analysis of Raman, EDX and XPS spectra confirms the efficient polymer deposition and the presence of Prussian Blue species embedded in the pEDOT matrix. TiO_2/pEDOT:Fehcf is characterised by a much higher charging current when compared to pure titania and exhibits reversible redox behaviour typical for Prussian blue activity. The current generated by heterojunction under solar simulated radiation is 4.72 times higher than the one registered for titania at +0.8 V that was mainly attributed to Fermi level alignment both of n and p element. Importantly, the combination of ordered titania and polymer containing inorganic species exhibits high stability during the electrochemical and photoactivity test that facilitates long-term usage of prepared heterojunction in prototype devices. This work was financially supported by the Polish National Science Center: Grant no. 2012/07/D/ST5/02269.

References

1 P. Roy, S. Berger and P. Schmuki, *Angew. Chem. In Ed.*, 2011, **50**, 2904.

2 A. Matsuda, S. Sreekantan and W. Krengvirat, *J. Asian. Ceram. Soc.*, 2013, **1**, 203.

3 K. Siuzdak, M. Szkoda, M. Sawczak and A. Lisowska-Oleksiak, *New J. Chem.*, 2015, **39**, 2741.

4 M. Dobbelin, R. Tena-Zaera, P.M. Carrasco, J.R. Sarasua, G. Cabanero and D. Mecerreyes, *J. Polym. Sci. A Polym. Chem.*, 2010, **48**, 4648.

5 Y. Kia, P. Xiao, H. He, J. Yao, Z. Wang, Y. Li, *Appl. Surf. Sci.*, 2012, **258**, 6627.

6 X. Li, W. Teng, Q. Zhao, l. Wang, *J. Nanopart. Res*., 2011, **13**, 6813.

7 S. Xie, M. Gan, L. Ma, Z. Li, J. Yan, H. Yin, X. Shen, F. Xu, J. Zheng, J. Zhang and J. Hu, *Electrochim. Acta,* 2014, **120**, 408.

8 C. Janaky, N.R. de Tacconi, W. Chanmanee and K. Rajeshwar, *J. Phys. Chem*. C, 2012, **116**, 19145.

9 Z. Wang, P. Xiao, L. Qiao, X. Meng, Y. Zhang, X. Li and F. Yanf, *Physica B*, 2013, **419**, 51.

10 S. Palmas, M. Mascia, A. Vacca, J. Llanos and E. Mena, *RSC Adv*., 2014, **4**, 23957.

11 K. Luo, Y. Ma, H. Wang and J. Chen, *Electrochim. Acta*, 2015, 167, 119.

12 Y. Jia, P. Xiao, H. He, J. Yao, F. Liu, Z. Wang and Y. Li, *Appl. Surf. Sci.*, 2012, **258**, 6627.

13 M. Ciabocco, M. Berrettoni, D.F. Martino Chillura and M. Giorgetti, *Solid State Ionics,* 2014, **259**, 53.

14 N.R. de Tacconi, K. Rajeshwar and R.O. Lezna*, Electrochim. Acta*, 2000, **45**, 3403.

15 I.A. Rutkowska, M. Skunik, K. Miecznikowski and P.J. Kulesza, *ECS Trans*., 2008, **13**, 185.

16 D. Oyarzun, R. Cordova, R. Henriquez, R. Schrebler, R.E. Marotti, E. Munoz, *J. Electroanal. Chem*., 2015, **740**, 75.

17 C. Janaky, G. Bencisik, A. Racz, C. Visy, N.R. de Tacconi, W. Chanmanee and K. Rajeshwar, *Langmuir*, 2010, **26**, 13697.

18 Y. Jia, P. Xiao, H. He, J. Yao, F. Liu, Z. Wang and Y. Li, *Appl. Surf. Sci*., 2012, **258**, 6627.

19 X. Yang, L. Chi, C. Chen, X. Cui and Q. Wang, *Physica E,* 2015, **66**, 120.

20 G. Zhang, G. Kim, W Choi, *Energy Environ. Sci*., 2014, **7**, 954.

21 K. Itaya, H. Akahoshi and S. Toshima, *J. Electrochem. Soc*., 1982, **129**, 1498.

22 K. Siuzdak, M. Szkoda, A. Lisowska-Oleksiak, J. Karczewski and J. Ryl, *RSC Adv*., 2016, **6**, 33101.

23 A. Lisowska-Oleksiak and A.P. Nowak, *J. Power Sources,* 2007, **173**, 829.

24 M. Datta and A. Datta, *J. Phys. Chem.,* 1990, **94**, 8203.

25 A. Lisowska-Oleksiak, A.P. Nowak, M. Wilamowska, M. Sikora, W. Szczerba and Cz. Kapusta, *Synthetic Metals*, 2010, **160**, 1234.

26 W. Macyk, K. Szaciłowski, H. Stochel, M. Buchalska, J. Kuncewica and P. Łabuz, *Coord. Chem. Rev*., 2010, **254**, 2687.

27 N.R. de Tacconi, K. Rajeshwar and R.O. Lezna, *Chem. Mater*., 2003, **15**, 3046.

28 A. Lisowska-Oleksiak, A.P. Nowak and V. Jasulaitiene, *Electrochem. Comm*., 2006, **8**, 107.

29 S. Boursiquot, M. Mullet, M. Abdelmoula, J.M. Genin and J.J. Ehrhardt, *Phys. Chem. Mater*., 2001, **28**, 600.

30 X. Chen and S.S. Mao, *Chem. Reviews*, 2007, **107**, 2891.

31 S. Garreau, G. Louarn and J. Buisson, *Macromolecules*, 1999, **32**, 6807.

32 A. Lisowska-Oleksiak, M. Wilamowska, V. Jasulaitiene, *Electrochim. Acta*, 2011, **56**, 3626.

33 K. Szaciłowski, W. Macyk and G. Stochel, *J. Mater. Chem*., 2006, **16**, 4603.

34 J. Chen, Z. Xia, H. Li, Q. Li, and Y. Zhang, *Electrochem. Acta,* 2014, **120**, 408.

35 F. Ricci and G. Palleschi, *Biosensors Bioelectr*., 2005, **21**, 389.

36 K. Itaya, T. Ataka, S. Toshima and T. Shinohara, *J. Phys. Chem*., 1982, **56**, 2415.

37 J. Bobacka, A. Lewenstam and A. Ivaska, J. *Electroanal. Chem*., 2000, **489**, 17.

38 D. Oyarzun, R. Cordova, R. Henriquez, R. Schrebler, R.E. Marotti and E. Munoz, *J. Electroanal. Chem*., 2015, **740**, 75.

39 Janaky et al., *J. Phys. Chem. C,* 2012, **116**, 4234.

40 H. Liang, X. Li, *Appl. Catal. B Envioron*., 2009, **86**, 8.

41 Y. Jia, P. Xiao, H. He, J. Yao, F. Liu, Z.Wang and Y. Li, *Appl. Surf. Sci*., 2012, **258**, 6627.

42 D. Oyarzun, R. Cordova, R. Henriquez, R. Schrebler, R.E. Marotti and E. Munoz, *J. Electroana. l Chem*., 2015, **740**, 75.

43 K. Szaciłowski, W. Macyk, M. Hebda and G. Stochel, *Chem. Phys. Chem*., 2006, **7**, 2384.

44 H.N. Gosh, J.B. Ashbury, Y. Weng, T. Lian, J. Phys. Chem. B, 1998, 102, 10208.

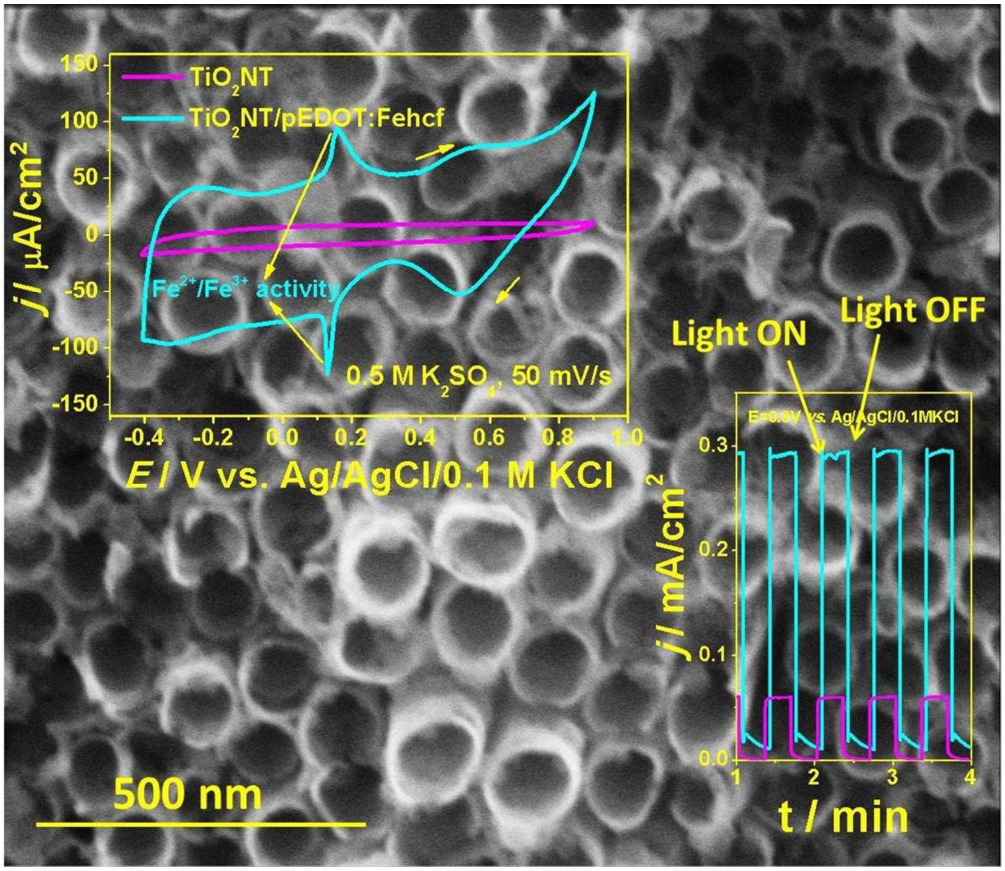

101x86mm (300 x 300 DPI)